Variable-Resolution Machine Learning for Rapid Multi-Criterial Antenna Design

Anna Pietrenko-Dabrowska[1[0000-0003-2319-6782]] and Slawomir Koziel[2,1[0000-0002-9063-2647]],

[1] Faculty of Electronics Telecommunications and Informatics, Gdansk University of Technology, Narutowicza 11/12, 80-233 Gdansk, Poland
anna.dabrowska@pg.edu.pl
[2] Engineering Optimization & Modeling Center, Department of Engineering, Reykjavík University, Menntavegur 1, 102 Reykjavík, Iceland
koziel@ru.is

Abstract. This research introduces a new technique for reduced-cost electromagnetic (EM)-driven multi-objective antenna optimization. Our approach employs artificial neural networks (ANNs) to build a surrogate model of antenna frequency characteristics, acting as a fast predictor providing multiple candidate Pareto-optimal solutions per iteration. The surrogate is refined within a machine-learning framework that leverages accumulated EM simulation data. Computational efficiency is enhanced by incorporating variable-fidelity EM simulations. Verification experiments underscrore competitive performance of our method, which requires only two hundred high-resolution EM analyses to complete the MO process. This represents 40% acceleration due to using variable-fidelity models and 90% speedup over traditional single-model surrogate-assisted methods. Our method is also shown competitive concerning design quality.

Keywords: Computer-aided design, antenna engineering, multi-objective optimization, machine learning, EM simulation, variable-fidelity models.

1 Introduction

Antennas belong to critical building blocks of wireless communication systems [1], [2]. Satisfying strict performance demands often results in complex structures requiring accurate electromagnetic (EM) analysis for reliable characterization, which is computationally costly. Furthermore, antenna development must balance multiple objectives: practical designs must establish trade-offs between different goals. Identifying these compromise solutions necessitates multi-objective optimization (MO) [3]. Yet, majority of existing procedures are limited to scalar cost functions [4], necessitating objective aggregation to enable multi-objective optimization (MO) [5].

Extensive data concerning trade-off solutions, normally generated as Pareto sets [6], is of high practical value. Predominant MO tools are bio-inspired algorithms that render the complete family of Pareto-optimal solutions in one algorithm execution. Notwithstanding, their applicability to handling EM simulation models is impeded by exceptionally poor cost efficiency. Practical EM-driven MO is often accomplished using surrogate modeling methods [7]. Therein, most computations are delegated to a fast replacement model. Popular modeling techniques include kriging, neural networks, and Gaussian process regression [8], [9]. The surrogate can be constructed beforehand [10] or iteratively during the optimization run, as in the machine learning (ML) frameworks [11]. The candidate designs identified by

ICCS Camera Ready Version 2025
To cite this paper please use the final published version:
DOI: 10.1007/978-3-031-97635-3_21

optimizing the surrogate are validated through EM analysis; the acquired EM data is employed to refine the metamodel. The work [12] provides a review of recent machine learning approaches to MO of antennas. The bottleneck of surrogate-based procedures is building the data-driven model. It is challenging in higher-dimensional spaces or if the spatial extent of the search space is vast. Domain confinement enables addressing dimensionality-related issues. One way is to identify the extreme non-dominated solutions (optimized for individual objectives) and constrain the domain to the smallest interval encapsulating these designs [13]. Constructing the model in the region encompassing high-quality designs, e.g., determined using pre-screening, is another option [14].

This study suggests a novel approach to improved-efficacy antenna MO. Our methodology is an ML algorithm utilizing an artificial neural network (ANN) surrogate. Multiple infill points are rendered in each iteration. The EM data acquired at the candidate designs is used to refine the metamodel. Reduction of the running costs is achieved by utilizing variable-fidelity EM analysis. Extensive verification reveals superior performance of the presented MO over benchmark methodologies. The typical cost of our algorithm corresponds to about 200 high-fidelity EM simulations. It also generates higher-quality Pareto sets compared to the benchmark regarding spatial extent and the Pareto dominance relation. The original contributions of this research include: (i) the development of an ML procedure employing ANN surrogates for high-efficacy MO of antennas, (ii) enhancing the cost efficiency of the search by incorporating multi-resolution EM analysis, (iii) and (iii) the implementation of the entire MO framework and demonstrating its performance using challenging test cases.

2 Multi-Criterial Design by Machine Learning

This part of the paper elaborates on the proposed MO algorithm. Problem statement is followed by an outline of the multi-fidelity EM models, the ANN surrogate, and a description of the machine-learning based MO procedure.

2.1 Problem Statement. Variable-Resolution EM Models

Let $\boldsymbol{F}(\boldsymbol{x}) = [F_1(\boldsymbol{x})\ F_2(\boldsymbol{x})\ \ldots\ F_{Nobj}(\boldsymbol{x})]^T$ be a vector of design goals, all to be minimized, where $\boldsymbol{x} = [x_1\ \ldots\ x_n]^T$ represents decision variables. Multi-objective optimization (MO) is understood as finding the Pareto set, a discrete representation of the Pareto front X_P containing all globally non-dominated designs w.r.t. the dominance relation [15]. The designs in X_P are the best available compromises between the objectives of interest.

MO tasks are normally solved using bio-inspired algorithms, which is rarely an option for EM-driven design due to high computational costs. The method proposed in here addresses these issues by incorporating ML, simultaneous rendition of multiple candidate solutions, and variable-resolution EM simulations. Design procedures typically involve a high-fidelity EM model $\boldsymbol{R}_f(\boldsymbol{x})$ that ensures sufficient reliability in evaluating antenna characteristics. To expedite the process we employ a range of lower-fidelity models $\boldsymbol{R}(\boldsymbol{x},L)$, where L is the control parameter governing the discretization density of the antenna under design. The lowest-fidelity model, $\boldsymbol{R}_c(\boldsymbol{x}) = \boldsymbol{R}(\boldsymbol{x},L_{\min})$, is set up to ensure that the EM simulation outputs render all relevant features of the antenna responses, whereas $\boldsymbol{R}_f(\boldsymbol{x}) = \boldsymbol{R}(\boldsymbol{x},L_{\max})$ is set to ensure sufficient reliability (as per designer's requirements).

ICCS Camera Ready Version 2025
To cite this paper please use the final published version:
DOI: 10.1007/978-3-031-97635-3_21

2.2 Neural Network Surrogates

The primary surrogate model used by the proposed MO procedure is an artificial neural network (ANN). The first model is constructed using N_{init} random samples $\boldsymbol{x}_B^{(j)}$, $j = 1, \ldots, N_{init}$, allocated by Latin Hypercube Sampling (LHS), and EM simulation outcomes $\boldsymbol{R}(\boldsymbol{x},L_{\min})$. The ANN used is a multi-layer perceptron [16] with two hidden layers (ten neurons each), and a sigmoid activation function. The model is trained using the Levenberg-Marquardt algorithm [16]. The model's inputs are design variables $\boldsymbol{x}$; the outputs are frequency characteristics (e.g., $|S_{11}|$ or gain vs. frequency), cf. Fig. 1.

2.3 MO by Machine Learning

In this study, the MO process is iterative. In each iteration, the Pareto set is approximated by optimizing the current ANN metamodel with the help of a multi-objective evolutionary algorithm (MOEA) with floating-point representation, fitness sharing with adaptively adjusted niche size, a combination of intermediate and arithmetic crossover, multi-point elitism, and a termination condition based on a sufficient reduction of newly created Pareto-optimal solutions [17]. The population size is set to $N_P = 200$, crossover and mutation probabilities are $p_m = 0.8$ and $p_c = 0.1$.

The candidates are extracted from the current Pareto set generated using MOEA. The EM data is inserted to the training set to refine the surrogate. The infill points $\boldsymbol{x}_I^{(i.j)}, j = 1, \ldots, N_{infill}$, are chosen to be possibly close to the target levels $F_j = F_{2.\min} + (F_{2.\max} - F_{2.\min})(j-1)/(N_{infill} - 1)$ of the second objective, where $F_{2.\min}$ and $F_{2.\max}$ decide the span of the Pareto front ($N_{infill} = 10$). Enhancing the cost efficiency is realized by employing variable-fidelity EM analysis. The initial metamodel is built using the lowest-fidelity data ($L_{\min}$). During the process, the resolution is enlarged to $L_{\max}$ to ensure dependability. The resolution $L^{(i)}$ in the ith iteration is determined as

$$L^{(i)} = \min\left\{ L_{\max}, L_{\min} + (L_{\max} - L_{\min})\frac{i-1}{i - N_{transition}} \right\} \qquad (1)$$

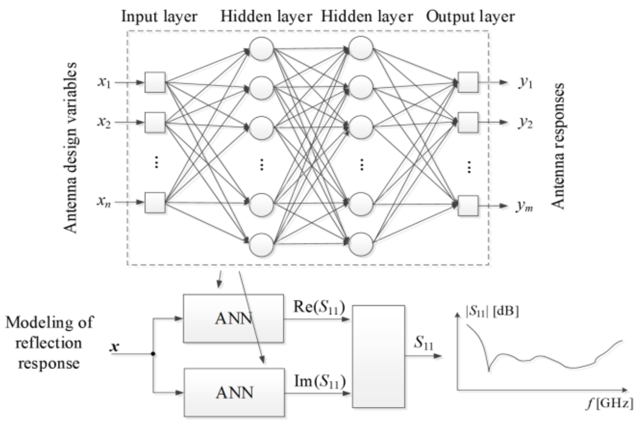

Fig. 1. The architecture of the ANN surrogate model utilized in this study is a multi-layer perceptron. The real and imaginary parts are modeled individually for complex responses. The outputs of the ANN are antenna characteristics at discrete set of frequencies f_1 through f_m.

ICCS Camera Ready Version 2025
To cite this paper please use the final published version:
DOI: 10.1007/978-3-031-97635-3_21

According to (1), the model resolution becomes $L_{\max}$ after $N_{transition}$, here, set to 5.

The strategy for updating the dataset used to build/refine the ANN surrogate is as follows. If only $\boldsymbol{R}_f$ is employed, all EM data acquired in the MO process is incorporated, including the initial set of samples $\boldsymbol{x}_B^{(j)}$, $j = 1, \ldots, N_{init}$, along with the infill points accumulated up to iteration i inclusive, i.e., $\boldsymbol{x}_I^{(k.j)}$, $k = 1, \ldots, i$, and $j = 1, \ldots, N_{infill}$. For variable-resolution approach, the lowest-fidelity samples are removed in each iteration, so that the overall number of data points does not exceed $2N_{init}$; however, if only $\boldsymbol{R}_f$ points are left, the dataset size may increase beyond $2N_{init}$.

The last component of the algorithm is the termination condition, which is founded on the sufficient resemblance of the Pareto fronts generated in subsequent iterations. The similarity metric is defined as

$$E_i = \left\| \boldsymbol{F}_{nondom}^{(i)} - \boldsymbol{F}_{nondom}^{(i-1)} \right\| \tag{2}$$

The algorithm is terminated if a moving average $E_{a.i} < \varepsilon$ (here, we set $\varepsilon = 1$), where

$$E_{a.i} = \frac{1}{i - \max\{1, i - N_a + 1\} + 1} \sum_{k=\max\{1, i-N_a+1\}}^{i} E_k \tag{3}$$

Using (3) enables smoothing fluctuations of E_i caused by the stochastic components in the optimization routine (specifically, MOEA).

2.4 Complete Framework

The flow diagram of the complete suggested MO procedure is illustrated in Fig. 2. There are several stages involved, which include the initial sampling, building the ANN metamodel, the machine learning optimization loop with iterative generation of multiple infill points, and metamodel refinement, as well as model management process adjusting the EM analysis fidelity during the search operation. The first stages are executed with the lowest-resolution EM analysis ($L_{\min}$), which is gradually increased so that the final dataset only contains high-fidelity samples ($L_{\max}$).

3 Results

This part of the manuscript showcases the operation of the proposed MO technique based on two antennas and juxtaposition to several benchmark algorithms.

3.1 Test Problems

Consider Antennas I and II illustrated in Fig. 3. Antenna I is realized on RF-35 substrate ($\varepsilon_r = 3.5$, $h = 0.762$ mm). The design variables are $\boldsymbol{x} = [L_0\ dR\ R\ r_{rel}\ dL\ dw\ Lg\ L_1\ R_1\ dr\ c_{rel}]^T$, the feed line width is $w_0 = 1.7$ (dimensions in mm). Antenna II is realized on RT6010 substrate ($\varepsilon_r = 10.2$, $h = 0.635$ mm) and its design variables are $\boldsymbol{x} = [s_1\ s_2\ v_1\ v_2\ u_1\ u_2\ u_3\ u_4]^T$; other parameters are $w_1 = w_3 = w_4 = 0.6$, $w_2 = 1.2$, $u_5 = 1.5$, $s_3 = 3.0$ and $v_3 = 17.5$. The EM models are simulated in CST Microwave Studio with the model fidelity controlled using lines-per-wavelength ($L = LPW$). The range of L for Antenna I is from $L_{\min} = 11$ (~210,000 mesh cells, simulation time 42 s) to $L_{\max} = 20$ (~2,300,000

ICCS Camera Ready Version 2025
To cite this paper please use the final published version:
DOI: 10.1007/978-3-031-97635-3_21

cells, 424 s). For Antenna II, we have L_{min} = 17 (~115,000 cells, 115 s) and L_{max} (~300,000 cells, 240 s). For Antenna I, the objectives are minimization of the substrate area (F_1) and minimization of the maximum reflection level within the operating band from 3.1 GHz to 10.6 GHz (F_2). For Antenna II, the goals are maximization of the end-fire gain (F_1), and minimization of the maximum $|S_{11}|$ within the operating range from 10 GHz to 11 GHz (F_2).

3.2 Verification Experiment Setup. Benchmark Techniques

The antennas of Fig. 3 are optimized using the suggested algorithm. The outcome is presented as the Pareto set encapsulating non-dominated parameter vectors extracted from the most recent EM dataset $\{\boldsymbol{x}_T^{(i.j)}\}$.

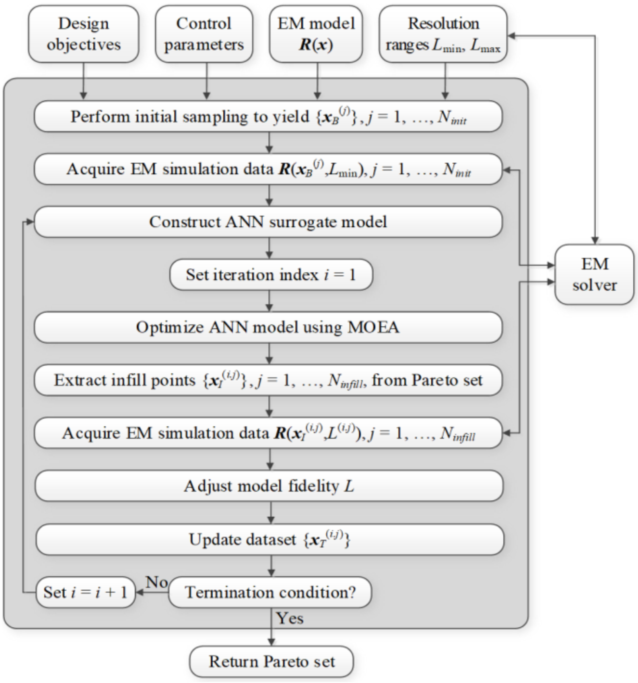

Fig. 2. Flow diagram of the proposed MO algorithm.

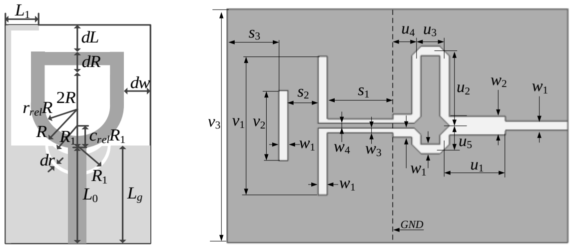

(a) (b)

Fig. 3. Verification devices: (a) Antenna I [18], (b) Antenna II [19].

ICCS Camera Ready Version 2025
To cite this paper please use the final published version:
DOI: 10.1007/978-3-031-97635-3_21

Our technique has been compared to three surrogate-assisted MO frameworks. Algorithms 1 and 2 are one-shot procedures (the metamodel is identified upfront and then optimized by means of MOEA). The difference between these methods is the surrogate modeling approach (kriging for Algorithm 1 and multi-layer perceptron for Algorithm 2). Both methods are run in two versions, different in the training dataset cardinality used to build the surrogate: 400 (version I), and 1600 (version II). Algorithm 3 is a single-objective version of the proposed method, where the optimization is carried out using the high-fidelity EM model. Furthermore, Algorithm 3 employs an accumulative dataset updating scheme: all candidate designs are inserted therein, and no samples are ever eliminated. These methods were specifically implemented for benchmarking.

3.3 Results and Discussion

Figures 4 and 5 show the Pareto sets produced by the suggested procedure and the benchmark techniques for Antenna I and II, respectively. The antenna responses for chosen Pareto optimal solutions can be found in Figs. 6. The design objectives and antenna responses are shown the pictures are evaluated using the respective high-fidelity EM models. The optimization costs have been gathered in Table 1. Note that only the expenses related to EM analysis are included as all other costs (ANN training, surrogate optimization using MOEA) are negligible compared to high-fidelity EM simulation (about four minutes for both Antenna I and II).

The results underscore remarkable performance of the proposed MO procedure regarding reliability and cost-efficiency. As indicated in Figs. 4 and 5, our framework yields significantly better Pareto sets than Algorithms 1 and 2. The reason is the relatively poor accuracy of the surrogate models used by these methods (kriging and ANN). The improvement observed for $N = 1600$ compared to $N = 400$ correlates with enhancing the surrogate's predictive power. For Antenna I, the relative root-mean-squared error (RRMSE) is reduced from around twenty to fifteen percent, whereas for Antenna II, RRMSE falls from eight to five percent. The non-dominated solution sets quality obtained by Algorithm 3 is comparable to the proposed method, demonstrating the advantages of machine learning over one-shot surrogate-assisted procedures.

Concerning cost efficiency (cf. Table 1), the introduced procedure is superior to all benchmark methods. The average CPU cost corresponds to only around 214 high-fidelity EM simulations, which corresponds to 48-percent speedup over Algorithms 1 and 2 (version I), 87-percent speedup over version II of Algorithms 1 and 2, and 38-percent acceleration over Algorithm 3.

Table 1. MO costs: proposed procedure versus benchmark algorithms

Algorithm		Optimization cost[#] Antenna I	Antenna II
This work (variable-fidelity ML with ANN surrogates)		150.4	264.4
Algorithm 1	N = 400 (version I)	400	400
	N = 1600 (version II)	1600	1600
Algorithm 2	N = 400 (version I)	400	400
	N = 1600 (version II)	1600	1600
Algorithm 3		320	340

[#] The cost is given in the number of $\boldsymbol{R}_f$ simulations. To compute the expenses for the proposed method, the relationship between the evaluation of time $\boldsymbol{R}_f$ and lower fidelity models is considered.

ICCS Camera Ready Version 2025
To cite this paper please use the final published version:
DOI: 10.1007/978-3-031-97635-3_21

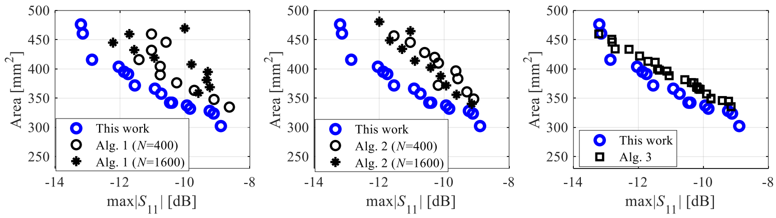

Fig. 4. Pareto sets found for Antenna I: proposed technique versus Algorithms 1, 2, and 3

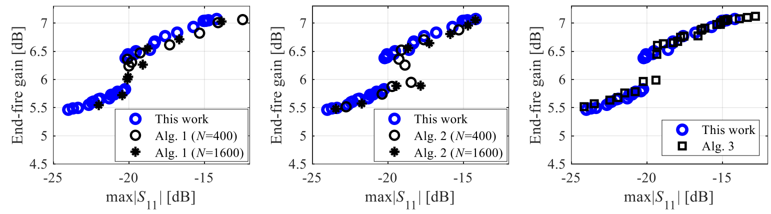

Fig. 5. Pareto sets obtained for Antenna II: proposed algorithm versus Algorithms 1, 2, and 3.

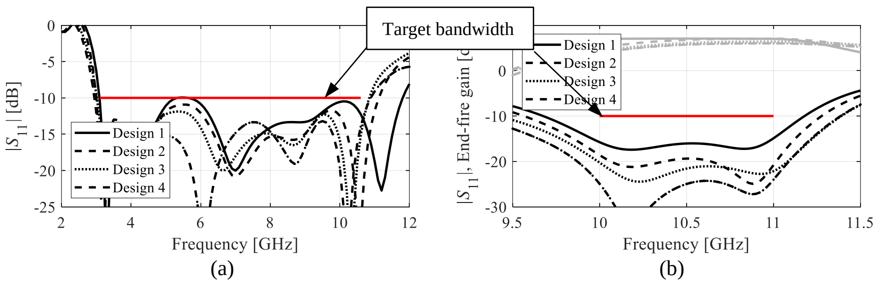

Fig. 6. Characteristics of Antennas I and II at the representative non-dominated designs found with the suggested algorithm: (a) Antenna I: Design 1 (A = 337 mm^2), Design 1 (A = 366 mm^2), Design 1 (A = 395 mm^2), Design 1 (A = 476 mm^2); (b) Antenna II: Design 1 (average gain 7.1 dB), Design 2 (average gain 6.5 dB), Design 3 (average gain 5.8 dB), Design 4 (average gain 5.5 dB).

The performance of our methodology makes it an appealing alternative to available MO algorithms. Its reliability and computational efficiency are accompanied by implementation simplicity and straightforward handling. Note these advantages were shown for test problems considerably more challenging than typically found in the MO-related literature.

4 Conclusion

This research suggested an alternative methodology for efficient multi-objective optimization (MO) of antennas, involving ANN metamodels and multi-fidelity EM simulations. Extensive validation demonstrates superior performance of the presented strategy regarding the solution quality and low running cost. These features are corroborated through benchmarking against diverse nature-inspired and ML frameworks. Future work will focus on extending our technique's applicability range for more challenging cases including higher-dimensional search spaces and increased numbers of objectives.

ICCS Camera Ready Version 2025
To cite this paper please use the final published version:
DOI: 10.1007/978-3-031-97635-3_21

Acknowledgment

This work is partially supported by the Icelandic Centre for Research (RANNIS) Grant 239858 and by the National Science Centre of Poland Grant 2020/37/B/ST7/01448.

References

1. Vinnakota, S.S., *et al.* Metasurface-assisted broadband compact dual-polarized dipole antenna for RF energy harvesting. IEEE Ant. Wireless Propag. Lett., **22**, 1912–1916 (2023)
2. Li, M., *et al.* Miniaturized slow-wave transmission line-based annular ring antenna with reconfigurable circular polarization. IEEE Ant. Wireless Propag. Lett., **22**, 1766–1770 (2023)
3. Koziel, S., Pietrenko-Dabrowska, A., Tolerance-aware multi-objective optimization of antennas by means of feature-based regression surrogates. IEEE Trans. Ant. Propag., **70**, 5636–5646 (2022)
4. Wang, J., Yang, X.S., Wang B.Z. Efficient gradient-based optimization of pixel antenna with large-scale connections. IET Microwaves Ant. Prop., **12**, 385–389 (2018)
5. Koziel, S., Pietrenko-Dabrowska, A., Mahrokh M. On decision-making strategies for improved-reliability size reduction of microwave passives: intermittent correction of equality constraints and adaptive handling of inequality constraints. Knowledge-Based Syst., **255**, paper no. 109745 (2022)
6. Mirjalili, S., Dong, J.S. Multi-Objective Optimization using Artificial Intelligence Techniques. Springer Briefs in Applied Sciences and Technology, New York (2019)
7. Easum, J.A., *et al.* Efficient multi-objective antenna optimization with tolerance analysis through the use of surrogate models. IEEE Trans. Ant. Prop., **66**, 6706–6715 (2018)
8. de Villiers, D.I.L., *et al.* Multi-objective optimization of reflector antennas using kriging and probability of improvement. Int. Symp. Ant. Prop., San Diego, USA, 985–986 (2017)
9. Dong, J., Qin, W., Wang M. Fast multi-objective optimization of multi-parameter antenna structures based on improved BPNN surrogate model. IEEE Access., **7**, 77692–77701 (2019)
10. De Melo, M.C., Santos, P.B., Faustino, E., Bastos-Filho, C.J.A., Sodré A.C. Computational intelligence-based methodology for antenna development. IEEE Trans. Ant. Propag., **10**, 1860–1870 (2022)
11. Nouri, M., Aghdam, S.A., Jafarieh, A., Mallat, N.K., Jamaluddin, M.H., Dor-Emami M. An optimized small compact rectangular antenna with meta-material based on fast multi-objective optimization for 5G mobile communication. J. Comp. Electr., **20**, 1532–1540 (2021)
12. Sarker, N., Podder, P., Mondal, M.R.H., Shafin, S.S., Kamruzzaman, J. Applications of machine learning and deep learning in antenna design, optimization, and selection: a review. IEEE Access., **11**, 103890–103915 (2023)
13. Koziel, S., Pietrenko-Dabrowska, A. Performance-driven surrogate modeling of high-frequency structures. Springer, New York (2020)
14. Pietrenko-Dabrowska, A., Koziel, S., Accelerated multi-objective design of miniaturized microwave components by means of nested kriging surrogates. Int. J. RF & Micr. CAE (2020)
15. Deb, K., Multi-Objective Optimization Using Evolutionary Alg. Wiley, New York (2001)
16. Vang-Mata, R. (Ed.), Multilayer perceptrons, Nova Science Pub. Inc. (2020)
17. Fonseca, C.M., Fleming, P.J. Multiobjective optimization and multiple constraint handling with evolutionary algorithms–Part I: a unified formulation. IEEE Trans. Syst. Man Cybernetics: Part A: Syst. Humans, **28**, 26–37 (1998)
18. Alsath, M.G.N., Kanagasabai, M., Compact UWB monopole antenna for automotive communications. IEEE Trans. Ant. Prop., **63**, 4204–4208 (2015)
19. Kaneda, N., Deal, W.R., Qian, Y., Waterhouse, R., Itoh T. A broad-band planar quasi Yagi antenna. IEEE Trans. Antennas Propag., **50**, 1158–1160 (2002)

ICCS Camera Ready Version 2025
To cite this paper please use the final published version:
DOI: 10.1007/978-3-031-97635-3_21